JURNAL KIMIA VALENSI

p-ISSN: 2460-6065; e-ISSN: 2548-3013

Journal homepage: https://journal.uinjkt.ac.id/index.php/valensi

Research Article

Synthesis of 3-(4-Hydroxy-3-Methoxyphenyl)-1-(2-Hydroxyphenyl)-Propenone as a Colorimetric Chemosensor for Hydrogen Phosphate Anions

Arfiani Nur[1,2], Bambang Purwono[3], Herlina Rasyid[1], Ummi Zahra[2], Aisyah[2], Artati[4], Andi N. Fitriani[5], Fadliah[6] , M.Yasser[7], Muharram[8], Paulina Taba[1], Indah Raya[1], Abdul W. Wahab[1], Nunuk H. Soekamto[1*]

[1]Department of Chemistry, Faculty of Mathematics and Natural Sciences, Hasanuddin University, Makassar, 90245, Indonesia
[2]Department of Chemistry, Faculty of Science and Technology, Alauddin State Islamic University, Makassar, 92118, Indonesia
[3]Department of Chemistry, Faculty of Mathematics and Natural Sciences, Gadjah Mada University, Yogyakarta, 55281, Indonesia
[4]Department of Health Analyst, Makassar Ministry of Health Polytechnic, Makassar, 90222, Indonesia
[5]Department of Chemistry, Faculty of Science, Universitas Muhammadiyah Bulukumba, Bulukumba, 92513, South Sulawesi, Indonesia
[6]Department of Mining Engineering, Faculty of Earth and Energy Technology, Universitas Trisakti, Jakarta, 11450, Indonesia
[7]Department of Chemical Engineering, Politeknik Negeri Ujung Pandang, Makassar, 90245, South Sulawesi, Indonesia
[8]Department of Chemistry, Faculty of Mathematics and Natural Sciences, Universitas Negeri Makassar, Makassar, 90224, South Sulawesi, Indonesia

[*]Email: nunukhariani@unhas.ac.id

Article Info

Received: Sept 12, 2026
Revised: May 30, 2026
Accepted: May 31, 2026
Online: June 6, 2026

Citation:
Nur, A., Purwono, B., Rasyid, H., Zahra, U., Aisyah., Artati., Fitriani, A. N., Fadliah., Yasser, M., Muharram., Taba, P., Raya, I., Wahab, A. W., Soekamto, N. H. (2026). Synthesis of 3-(4-Hydroxy-3-Methoxyphenyl)-1-(2-Hydroxyphenyl)-Propenone as a Colorimetric Chemosensor for Hydrogen Phosphate Anions. *Jurnal Kimia Valensi*, 12(1), 144-155.

Doi: 10.15408/jkv.v12i1.46467

Abstract

Hydrogen phosphate is an important anion in environmental and biological systems; however, its excessive presence in water can contribute to eutrophication and water quality degradation. The synthesis and application of 3-(4-hydroxy-3-methoxyphenyl)-1-(2-hydroxyphenyl)-propenone (HMPP) as a colorimetric chemosensor for hydrogen phosphate (HPO_4^{2-}) anions have been investigated. HMPP was synthesized via Claisen–Schmidt condensation of vanillin and 2-hydroxyacetophenone, obtained in 34% yield of the target compound. The colorimetric response of HMPP was evaluated toward various anions, including F^-, Cl^-, Br^-, CN^-, HPO_4^{2-}, and CO_3^{2-}. The results showed that HMPP exhibited a distinct response toward HPO_4^{2-}; however, the presence of other anions caused varying degrees of interference, with CO_3^{2-} showing minimal effect, while Cl^-, CN^-, and Br^- reduced the response to a greater extent. This behavior is attributed to hydrogen-bonding interactions between HMPP and HPO_4^{2-}, which enhance intramolecular charge transfer (ICT). The applicability of HMPP was further evaluated in spiked tap water samples, demonstrating satisfactory recovery in the range of 105.47–107.50%, indicating acceptable accuracy and reliability. Therefore, HMPP demonstrates potential as a colorimetric chemosensor for hydrogen phosphate anions in water samples.

Keywords: Colorimetric chemosensor, Claisen–Schmidt condensation, hydrogen phosphate, 3-(4-hydroxy-3-methoxyphenyl)-1-(2-hydroxyphenyl)-propenone

1. INTRODUCTION

The detection and monitoring of anions play a vital role in various fields, including environmental science, biology, and industrial processes, as these species are involved in numerous chemical and biochemical systems [1–4]. Among them, the hydrogen phosphate anion (HPO_4^{2-}) is an essential component in biological processes, such as energy transfer (e.g., ATP hydrolysis) and cellular signaling. However, excessive levels of phosphate species in aquatic systems can lead to serious environmental problems, particularly eutrophication, which disrupts ecosystem balance and water quality [5,6]. Therefore, the development of efficient methods for the detection of HPO_4^{2-} is of significant importance.

Colorimetric chemosensors offer an effective and practical approach for anion detection due to their simplicity, cost-effectiveness, and ability to provide direct visual responses without the need for sophisticated instrumentation [7,8]. Among various molecular frameworks, chalcone derivatives have attracted considerable attention as promising platforms for colorimetric sensing owing to their extended π-conjugated systems and tunable electronic and photophysical properties [9]. The incorporation of functional groups such as hydroxyl and methoxy substituents can enhance interactions with target anions through hydrogen bonding and modulation of electronic properties, leading to measurable optical responses [10].

Recent advances in anion sensing have focused on organic colorimetric chemosensors based on conjugated chromophores capable of selective recognition through hydrogen bonding and charge-transfer mechanisms [1,7,10]. Chalcone-based systems have been reported as promising sensing platforms due to their facile synthesis, structural tunability, and strong optical responses toward various ions and anions [9–12]. Meanwhile, recent phosphate-sensing strategies include coordination polymers, metal-complex sensors, MOF-based colorimetric platforms, electrochemical sensors, and ratiometric fluorescent systems [13–24]. Nevertheless, many reported phosphate sensors still involve metal-based frameworks, complex instrumentation, or limited practical application in real water samples. Therefore, the development of a simple chalcone-based colorimetric chemosensor with practical applicability for HPO_4^{2-} detection remains important.

Hydroxy-substituted chalcones, in particular, are known to exhibit strong responses toward basic anions through mechanisms such as hydrogen bonding and deprotonation, which can induce significant changes in their absorption behavior. These interactions often result in intramolecular charge transfer (ICT) enhancement, giving rise to distinct spectral and colorimetric responses. Such characteristics make chalcone-based systems suitable candidates for the development of simple and efficient anion sensors.

In addition to sensing applications, chalcone derivatives bearing hydroxyl, methoxy, and carbonyl functional groups have also been explored in molecularly imprinted polymers (MIPs), where these functional groups facilitate specific interactions such as hydrogen bonding, dipole–dipole interactions, and π–π interactions. Previous studies have demonstrated that MIPs based on similar compounds exhibit high adsorption capacity and good recognition ability toward target molecules, supporting their broader applicability in separation and sensing technologies [11,12]. Furthermore, these compounds have been produced and commercialized in various isomeric forms, indicating their industrial relevance [25,26].

In this study, we report the synthesis and application of 3-(4-hydroxy-3-methoxyphenyl)-1-(2-hydroxyphenyl)-propenone (HMPP), a chalcone derivative, as a colorimetric chemosensor for hydrogen phosphate (HPO_4^{2-}) anions. The structural features of HMPP are designed to facilitate interaction with HPO_4^{2-}, resulting in observable optical responses. The sensing performance of HMPP, including its response behavior, interference from competing anions, and applicability in water samples, is systematically evaluated. This study highlights the potential of chalcone-based systems as simple and effective platforms for hydrogen phosphate detection.

2. RESEARCH METHODS

Materials

The synthesis of 3-(4-hydroxy-3-methoxyphenyl)-1-(2-hydroxyphenyl)-propenone used the following materials: vanillin ($C_8H_8O_3$, Macklin Biochemical Co., China), 2-hydroxyacetophenone ($C_8H_8O_2$, Macklin Biochemical Co., China), potassium hydroxide (KOH, Merck), hydrochloric acid (HCl, Merck), methanol (CH_3OH, Merck), chloroform ($CHCl_3$, Merck), petroleum ether (Merck), pH indicator paper (Merck), thin layer chromatography (TLC) plate (Merck), Whatman filter paper, and distilled water. Meanwhile, the materials used for chemosensory activities are DMSO (Merck), ethanol (Merck), ethyl acetate (Merck), sodium fluoride (NaF, Macklin Biochemical Co., China), sodium chloride (NaCl, Merck), sodium bromide (NaBr, Macklin Biochemical Co., China), sodium cyanide (NaCN, Merck), disodium hydrogen phosphate (Na_2HPO_4, Merck) and sodium carbonate (Na_2CO_3, Merck).

Synthesis method of 3-(4-hydroxy-3-methoxyphenyl)-1-(2-hydroxyphenyl)-propenone

The experimental method (Scheme 1) was modified by previous reports [27]. 2-Hydroxyacetophenone (5 mmol, 0.680 g) was dissolved in 7.5 mL of absolute ethanol and homogenized using a magnetic stirrer. Dropwise, 12.5 mL of 6N KOH was added, and the mixture was stirred for 10 minutes. Vanillin (5 mmol, 0.760 g) was then added, and the reaction was irradiated with domestic microwave (Kirin, Indonesia) at 187 W for 10 minutes. Reaction progress was monitored by TLC.

The mixture was left to stand for 24 hours, followed by the addition of 15 mL cold distilled water and neutralization with 10% HCl. Crystals formed were filtered using a Buchner funnel, washed, dried at room temperature, and weighed. Purity was confirmed by TLC using chloroform: petroleum ether (4:1) as the mobile phase.

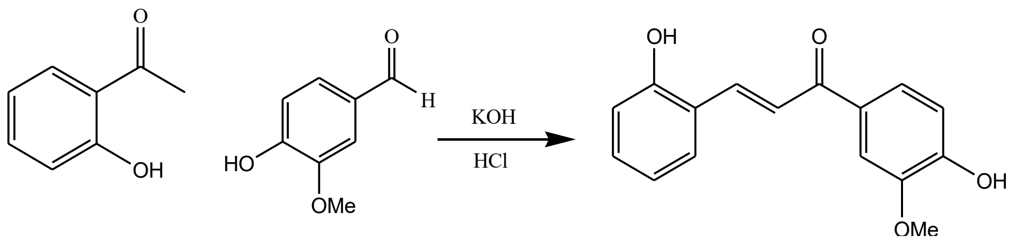

Scheme 1. Synthesis route of HMPP via Claisen–Schmidt condensation

Chemical characterisation

The compounds were characterized using a Fourier Transform Infrared (FTIR) Spectrophotometer (Thermo Scientific Nicolet iS10), GC-MS (column: HP-5MS UI), ^{1}H-NMR (500 MHz, $CDCl_3$), and ^{13}C-NMR (500 MHz, $CDCl_3$). Melting point test using melting point apparatus. Colorimetric chemosensor activity was evaluated using UV-Vis Spectrophotometer (Varian Cary 50). GC–MS analysis was conducted using an HP-5MS UI column (30 m × 0.25 mm × 0.25 μm) with helium as the carrier gas (1.00 mL/min). The injector temperature was 250 °C (split ratio 10:1). The MS transfer line and ion source temperatures were set at 280 °C, and mass spectra were acquired in the range of m/z 40–500.

Yield (%) = 34%; mp = 150°C; ^{1}H-NMR (500 MHz, Methanol-d_4) δ_H (ppm): 7.71(*d*, 1H); 7.58 (*d*, 1H); 7.49 (*s*, 1H); 7.39 (*dd*, 1H); 7.32 (*s*, 1H) ; 7.22 (*d*, 1H) ; 7.13 (*s*, 1H) ; 7.08 (*d*, 1H); 6.96 (*d*, 1H) ; 3.97 (*s*, 3H). ; ^{13}C-NMR (125 MHz, Methanol-d_4) δ_C (ppm):197.16 (-Cq); 145.49 (-Cq); 129.85 (-CHalkene) ; 120.95(-Cq) ; 119.64 (-CHar) ; 114.97 (-CHar) ; 109.92(-CHar); 56.037 (-Cmethoxy); FTIR wavenumber (cm^{-1}) : 3421 (-OH); 1681 (-C=O) ;1606 and 1462 (C=Car) ; 1272 (C-O). GC–MS (EI): m/z calculated found 270.1. (See Figures S1–S4 Supporting Information).

The GC–MS chromatogram showed two major peaks with the same molecular ion at m/z 270, corresponding to relative areas of 60.42% and 28.85%. This result suggests the presence of two components with the same molecular mass, which may be attributed to possible isomeric forms or closely related chalcone-derived products. The melting point range showed a narrow difference of approximately 2 °C, indicating relatively consistent crystalline behavior after purification.

Colorimetric chemosensor activity

Solvatochromic test

To evaluate the solvatochromic properties of the compound, 1 mg of the sample was dissolved in 10 mL of various solvents, including ethyl acetate, ethanol, methanol, DMSO, and a DMSO-water mixture (3:2, v/v). The resulting solutions were visually examined for color changes. Subsequently, the UV-Vis absorption spectra of each solution (0.001%) were recorded within the range of 200–800 nm using a UV-Vis spectrophotometer, following the protocol described by Nur and Purwono (2017) [28].

Evaluation of Colorimetric Sensing Activity for Saturated Anions

To assess the compound's activity as a colorimetric sensor for anions, 1 mL of its solution (0.001%) was prepared in different solvents (ethyl acetate, ethanol, acetonitrile, methanol, DMSO, and DMSO-water (3:2, v/v)) and transferred into individual vials. Subsequently, 50 μL of saturated aqueous solutions of sodium salts of F^-, Cl^-, Br^-, CN^-, HPO_4^{2-}, and CO_3^{2-} were added to each vial. The resulting solutions were observed for any changes in color, and these changes were documented as per the method described by Nur and Purwono (2017) [28].

Determination of Equivalence Point and Detection Limit

For the determination of the equivalence point and detection limit, 0.01 mmol of the compound was dissolved in 1 mL of the solvent that exhibited the most significant wavelength shift in the solvatochromic test. A 20 μL aliquot of this solution was diluted with 1 mL of the same solvent, followed by the incremental addition of 20, 40, 80, 100, 200, 500, 1000, and 2000 μL of a 0.01 mmol solution of the anion that showed the most pronounced color change. After each addition, the UV-Vis absorption spectra of the mixture were recorded in the wavelength range of 200–800 nm using a UV-Vis spectrophotometer. The method was performed in accordance with the procedure outlined by Nur and Purwono (2017) [28].

Selectivity Study

HMPP (0.03 mmol) was dissolved in 3 mL of a DMSO:water mixture (3:2, v/v) to obtain a 10 mM stock solution, which was subsequently diluted to a 0.4

mM working solution. An aliquot (120 µL) of this solution was placed in a vial, and 190 µL of each anion solution (F^-, Cl^-, Br^-, and CO_3^{2-}; 10 mM, prepared by dissolving 0.1 mmol of the corresponding sodium salts in 10 mL of distilled water) was added, followed by the addition of 190 µL Na_2HPO_4 (10 mM). The mixtures were homogenized for several minutes, and the absorbance was then measured at 500 nm using a UV–Vis spectrophotometer.

Application of HMPP Chemosensor in Tap Water Samples

Tap water samples were collected from three different locations in Gowa Regency, Indonesia, and filtered prior to analysis to remove suspended particles. For the real sample test, 4.80 mL of each filtered tap water sample was transferred into a vial, followed by the addition of 100 µL of HMPP stock solution (1200 ppm) and 100 µL of HPO_4^{2-} standard solution (640 ppm). The final volume of the mixture was adjusted to 5.00 mL, resulting in final concentrations of 24 ppm HMPP and 12.8 ppm HPO_4^{2-}. The mixture was homogenized and allowed to stand for the optimum response time before analysis using the synthesized HMPP chemosensor. All measurements were performed in triplicate, and the obtained data were used to calculate the percentage recovery and relative standard deviation (RSD) to evaluate the accuracy and precision of the method in real tap water samples.

3. RESULTS AND DISCUSSION

Synthesis of 3-(4-hydroxy-3-methoxyphenyl)-1-(2-hydroxyphenyl)-propenone

The moderate yield (34%) obtained in this study may be influenced by several factors related to the structural characteristics of the reactants and the reaction conditions. The presence of hydroxyl and methoxy substituents on the aromatic rings can alter the electronic distribution of the starting materials through electron-donating effects, thereby affecting the electrophilicity of the carbonyl carbon and the overall efficiency of the Claisen–Schmidt condensation reaction. In addition, the hydroxyl groups may participate in intramolecular and intermolecular hydrogen bonding, which can reduce the reactivity of the reactants and potentially stabilize intermediate species during the reaction process. Steric effects arising from substituted aromatic rings may also hinder effective molecular interactions required for condensation. Furthermore, side reactions such as self-condensation, incomplete conversion of starting materials, or product loss during purification and recrystallization may contribute to the relatively low isolated yield. Similar moderate yields have been reported in related substituted chalcone syntheses, where yields in the range of 30–40% were attributed to substituent effects and purification losses [11,25,27]. Therefore, the obtained yield is still considered reasonable for hydroxy- and methoxy-substituted chalcone derivatives synthesized under comparable conditions.

The compound 3-(4-hydroxy-3-methoxyphenyl)-1-(2-hydroxyphenyl)-propenone was successfully synthesized through a Claisen-Schmidt condensation reaction between vanillin (4-hydroxy-3-methoxybenzaldehyde) and 2-hydroxyacetophenone under basic conditions. The resulting product was a yellow solid with a yield of 34% and a melting point of 150-152°C. FTIR spectral analysis confirmed the presence of key functional groups in the compound. The broad absorption band at 3421 cm^{-1} indicated O-H stretching vibrations from hydroxyl groups, while a strong peak at 1681 cm^{-1} corresponded to the C=O bond in the ketone group. Additional peaks at 1606 and 1462 cm^{-1} were attributed to C=C stretching vibrations in the aromatic rings, and a peak at 1272 cm^{-1} was consistent with C-O stretching vibrations from the methoxy group of vanillin. These findings validated the structure of the compound.

^1H-NMR analysis provided further confirmation of the compound's molecular structure. A singlet at δ_H 3.97 ppm indicated the presence of a methoxy proton ($-OCH_3$) at the para position relative to the hydroxyl group in the vanillin ring. Aromatic protons were observed in the range of δ_H 6.8–7.5 ppm, while a doublet at δ_H 7.5–7.7 ppm was associated with the vinyl proton (CH=CH) adjacent to the carbonyl group. Similarly, ^{13}C-NMR analysis confirmed the presence of carbon atoms consistent with the target structure. Signals at δ_C 56 ppm represented the methoxy carbon, while a strong signal at δ_C 197 ppm corresponded to the carbonyl carbon of the ketone group. Additional signals in the range δ_C 112–164 ppm were attributed to aromatic carbons, and vinyl carbons were observed at δ 129 and 145 ppm. These data collectively supported the successful synthesis of the compound with the intended molecular framework.

The ^{13}C NMR spectrum showed fewer observable signals than the expected number of carbon atoms, which may be attributed to overlapping aromatic carbon signals and low signal intensity. Nevertheless, the presence of key signals, including the carbonyl carbon around δ_C 195 ppm, aromatic/olefinic carbons in the range of δ_C 110–150 ppm, and the methoxy carbon around δ_C 56 ppm, supports the formation of the chalcone framework.

The results from FTIR, ^1H-NMR, and ^{13}C-NMR analyses confirmed the structure of 3-(4-hydroxy-3-methoxyphenyl)-1-(2-hydroxyphenyl)-propenone (**Figure 1**). The presence of key functional groups such as hydroxyl, methoxy, and carbonyl was clearly detected, aligning with the expected molecular design.

Similar chalcone derivatives have been widely investigated due to their diverse biological activities, including anticancer, antiviral, and antimicrobial properties[29,30]. Variations in substituents on the aromatic rings, particularly hydroxyl and methoxy groups, significantly influence their physicochemical and biological properties. Future research could focus on characterizing the compound's potential as a chemosensor or in other advanced applications in molecular recognition and materials science.

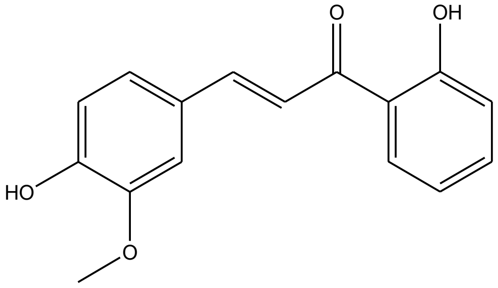

Figure 1. Chemical structure of 3-(4-hydroxy-3-methoxyphenyl)-1-(2-hydroxyphenyl)-propenone (HMPP)

Colorimetric chemosensor activity

Solvatochromic test

The UV–Vis absorption spectrum (**Figure 2**) shows two characteristic bands of chalcone systems: Band II in the UV region (π–π* transition of the benzoyl system) and Band I in the visible region (π–π* transition of the cinnamoyl system). The introduction of electron-donating groups such as hydroxyl and methoxy is expected to increase conjugation and intramolecular charge transfer (ICT), resulting in a red shift of the absorption maximum.

In the solvatochromic test, the compound was dissolved in various solvents to evaluate color changes resulting from interactions between the compound and the different solvent environments. The solvents used in this study were ethyl acetate, methanol, ethanol, DMSO, and a DMSO:water mixture with a 3:2 ratio. Observations revealed that the most significant color change occurred in DMSO (dimethyl sulfoxide). DMSO is well-known for its strong interaction capabilities with polar compounds due to its properties as an excellent polar aprotic solvent. The color observed in DMSO indicates an intense interaction between the test compound and the solvent, reflecting a significant difference in the solvation effect compared to other solvents. Solvatochromism arises from variations in the ability of solvents to stabilize the electronic states of a compound through solute-solvent interactions, such as dipole-dipole interactions, hydrogen bonding, or electron donor-acceptor interactions. Solvents with varying polarities and proton donor capabilities affect the compound's excitation energy differently, resulting in observable color changes. Ethyl acetate, a non-polar or slightly polar solvent, showed no significant color change, indicating weak interactions between the solvent and the test compound. Methanol and ethanol, both polar protic solvents capable of hydrogen bonding with the compound, exhibited moderate color changes. However, these changes were less pronounced compared to DMSO, suggesting that while solvent-solute interactions exist, they are not as strong as those observed with DMSO. As a polar aprotic solvent, DMSO effectively stabilizes the test compound through dipole-dipole interactions, leading to the most pronounced color changes[31]. This is because DMSO provides stronger solvation for polar compounds. In the DMSO:water (3:2) mixture, although the color change was less intense compared to pure DMSO, the mixture still produced adequate results. This mixture was chosen due to its relevance to real-world applications, particularly in aqueous environments commonly used in biological or analytical chemistry. DMSO enhances the compound's solubility in water while retaining some of the solvatochromic properties observed in pure DMSO.

Overall, while DMSO produced the most significant color change, this corresponds to observable changes in the UV–Vis absorption spectrum, including a shift in λmax. the DMSO:water mixture was selected for further applications due to its practical relevance, particularly in aqueous media often encountered in biological or analytical environments. This choice balances the strong solvation effects of DMSO with the compatibility of water-based systems, making the mixture suitable for applications in real contexts.

Evaluation of Colorimetric Sensing Activity for Saturated Anions and Cations

In this test, the chemosensor compound was evaluated against various saturated anions from their sodium salts, including F^-, Cl^-, Br^-, HPO_4^{2-}, CO_3^{2-}, and CN^- (**Figure 3**). The purpose of the test was to observe color changes resulting from specific interactions between the chemosensor compound and each anion. The most notable change occurred with the HPO_4^{2-} anion, where the chemosensor solution changed from light yellow to red. This indicates a very strong interaction between the chemosensor and the phosphate anion, leading to significant changes in the electronic structure and a corresponding dramatic color shift. Fluoride (F^-) induced a color change from light yellow to pink. Although less pronounced than the change with HPO_4^{2-}, the response to F^- suggests a reasonably strong specific interaction between F^- and the chemosensor's binding site. Carbonate (CO_3^{2-}) and cyanide (CN^-) both triggered a color change to orange. The orange color indicates moderate interactions between the chemosensor and these anions, with sufficient energy transitions to influence the solution's color. Chloride (Cl^-) and bromide (Br^-) anions, however, did not cause significant color changes. This suggests relatively weak interactions between the chemosensor and these anions, resulting in no substantial alteration of the compound's electronic structure.

Chemosensors function based on specific interactions between the binding sites within the compound and the target anions. The observed color changes are caused by electronic transitions within the chemosensor compound, influenced by the anion binding. Each anion exhibits unique chemical properties, such as size, charge, and hydrogen bonding ability, which determine the strength of its interaction with the chemosensor and the magnitude of the resulting color change. Among the tested anions, HPO_4^{2-} produced the most drastic color shift from light yellow to red, indicating a strong interaction. Phosphate is known for its high affinity for proton donors and its ability to act as a good ligand[32], forming robust interactions with the chemosensor and causing significant changes in the UV-Vis spectrum.

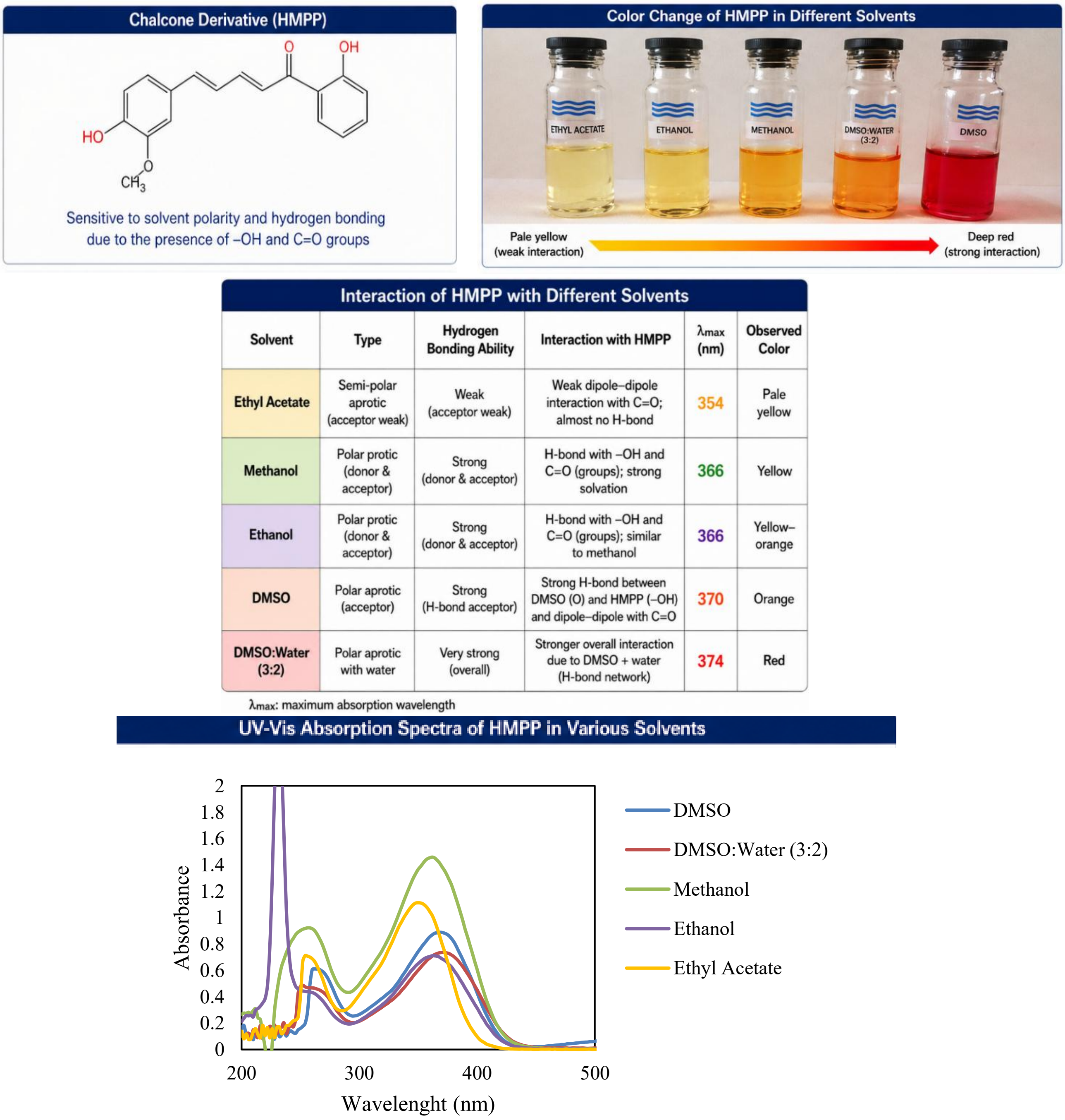

Chalcone Derivative (HMPP)

Sensitive to solvent polarity and hydrogen bonding due to the presence of –OH and C=O groups

Color Change of HMPP in Different Solvents

Interaction of HMPP with Different Solvents

Solvent	Type	Hydrogen Bonding Ability	Interaction with HMPP	λmax (nm)	Observed Color
Ethyl Acetate	Semi-polar aprotic (acceptor weak)	Weak (acceptor weak)	Weak dipole–dipole interaction with C=O; almost no H-bond	354	Pale yellow
Methanol	Polar protic (donor & acceptor)	Strong (donor & acceptor)	H-bond with –OH and C=O (groups); strong solvation	366	Yellow
Ethanol	Polar protic (donor & acceptor)	Strong (donor & acceptor)	H-bond with –OH and C=O (groups); similar to methanol	366	Yellow–orange
DMSO	Polar aprotic (acceptor)	Strong (H-bond acceptor)	Strong H-bond between DMSO (O) and HMPP (–OH) and dipole–dipole with C=O	370	Orange
DMSO:Water (3:2)	Polar aprotic with water	Very strong (overall)	Stronger overall interaction due to DMSO + water (H-bond network)	374	Red

λmax: maximum absorption wavelength

UV-Vis Absorption Spectra of HMPP in Various Solvents

Figure 2. Solvatochromic test results of 3-(4-hydroxy-3-methoxyphenyl)-1-(2-hydroxyphenyl)-propenone in various solvents at a concentration of 10 ppm

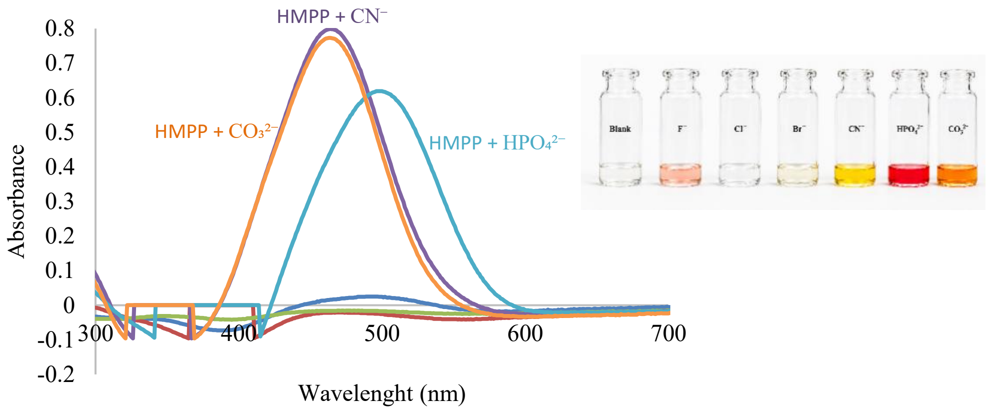

Figure 3. Colorimetric sensing activity of HMPP toward saturated anion solutions

Fluoride (F^-), as a small anion with a high charge density[33], also showed significant interaction, although the color change was limited to pink. F^- can form strong hydrogen bonds with hydrogen donor groups in the chemosensor, though its effect is less pronounced than that of HPO_4^{2-}. CO_3^{2-} and CN^- exhibited similar color changes to orange. While their interactions with the chemosensor were strong enough to induce a visible color change, the binding strength was still weaker than that of HPO_4^{2-} and F^-. Cyanide (CN^-), with its strong basic character, can also influenced the absorption spectrum of the chemosensor. Conversely, Cl^- and Br^- showed minimal or no color changes, indicating weak interactions with the chemosensor. This may be attributed to their larger size or their inability to strongly interact with the available binding sites.

In summary, HPO_4^{2-} demonstrated the strongest interaction with the chemosensor, followed by F^-, CO_3^{2-}, and CN^-, which elicited moderate responses. Cl^- and Br^- displayed weak interactions, resulting in negligible changes. These findings highlight the specificity of the chemosensor compound towards certain anions and provide insights into its potential application for selective anion detection.

Determination of Equivalence Point and Detection Limit

The sensitivity evaluation of the chemosensor toward hydrogen phosphate ions (HPO_4^{2-}) was performed using UV-Vis spectroscopy (**Figure 4**). Standard HPO_4^{2-} solutions with varying concentrations were prepared, and changes in absorbance at the maximum wavelength were analyzed. The calibration curve exhibited a linear relationship between HPO_4^{2-} concentration and absorbance over the range of 12–24 ppm, with a coefficient of determination (R^2) of 0.9301. This value indicates a moderately linear correlation between concentration and absorbance, although minor deviations from linearity may be attributed to factors such as solution instability or matrix interference.

The limit of detection (LOD) of the chemosensor was calculated using the standard approach, defined as three times the standard deviation of the blank signal divided by the slope of the calibration curve. From this calculation, the LOD was determined to be 0.19 ppm (2 μM). A comparison with previously reported phosphate sensors (**Table 1**) shows that fluorescence-based systems, particularly those incorporating nanomaterials or advanced platforms, can achieve detection limits in the nanomolar to submicromolar range. In contrast, UV–Vis and colorimetric sensors generally exhibit detection limits within the micromolar range. In this context, the proposed chemosensor, with a limit of detection of approximately 2 μM, demonstrates moderate to good sensitivity and is comparable to many reported UV–Vis-based systems. Although it does not reach the ultralow detection limits of fluorescence-based probes, the present method offers practical advantages, including operational simplicity, cost-effectiveness, and the use of readily accessible instrumentation. These features highlight its potential applicability for routine detection of HPO_4^{2-} in solution.

The stoichiometric relationship between HMPP and HPO_4^{2-} was investigated using Job's method of continuous variation (**Figure 5**). The maximum absorbance was observed at a mole fraction of approximately 0.25–0.30, suggesting a binding stoichiometry close to 1:2 (HMPP:HPO_4^{2-}). Although the maximum does not occur exactly at the theoretical value of 0.33, this deviation may be attributed to experimental limitations or partial complex formation in solution. Overall, the results indicate that one HMPP molecule interacts with two HPO_4^{2-} ions (**Figure 6**). For further studies, including binding constant determination, and pH-dependent UV–Vis investigations are recommended to fully elucidate the sensing mechanisms.

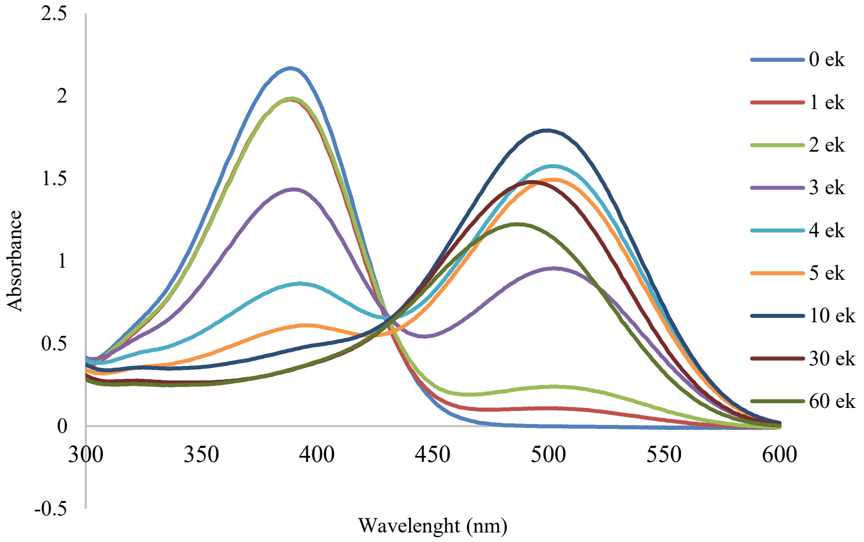

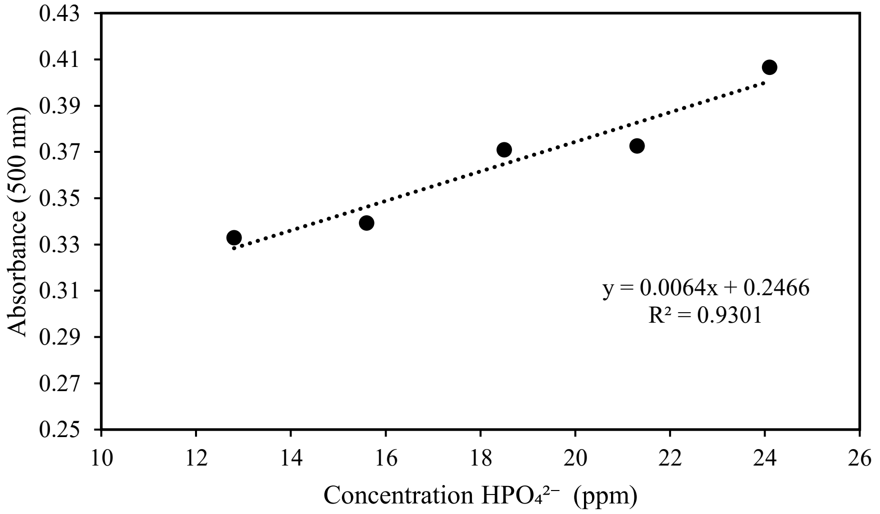

Figure 4. Linear regression curve showing the relationship between HPO_4^{2-} concentration (ppm) and HMPP absorbance response

Table 1. Comparison of representative phosphate (HPO_4^{2-}/PO_4^{3-}) sensors

Sensor System	Method	Linear Range (µM)	LOD (µM)	Medium	Selectivity	Ref
Eu-based coordination polymer	Fluorescence	~1–100	0.12	Aqueous	High	13
Zn^{2+} complex probe	Fluorescence	~1–50	0.31	DMSO	High	14
Indigo carmine–Cu^{2+}	Colorimetric	~1–100	0.071	H_2O/DMSO	Excellent	15
Fe^{3+} displacement sensor	Colorimetric	~5–200	0.36	Aqueous	High	16
MOF-808 (Zr/Ce)	Colorimetric	11–581	3.7	Aqueous	Moderate	17
Luminescent polymer sensor	Fluorescence	µM range	~0.1–1	Aqueous	High	18
Microfluidic analyzer	Colorimetric	0.2–10	0.015	Seawater	Very high	19
Aptamer-based electrochemical sensor	Electrochemical	µM range	~0.1–1	Aqueous	High	20
Ion-selective electrode	Potentiometric	µM–mM	~1–5	Aqueous	Moderate	21
Electrochemical microsystem	Electrochemical	µM range	~0.5–2	Seawater	Good	22
Fe_3O_4–FMN nanoprobe	Fluorescence	µM range	~0.1–0.5	Environmental water	High	23
POM@PMO electrode	Electrochemical	µM range	<1	Aqueous	High	24
This work	Colorimetric	126–252	~2.0	H_2O/DMSO	Moderate	This work

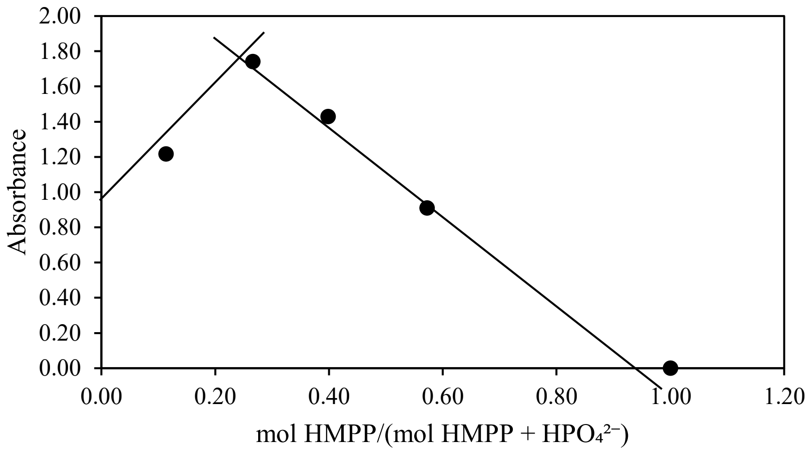

Figure 5. Job's plot of HMPP and HPO_4^{2-} obtained from UV–Vis absorbance measurements. The maximum absorbance occurs at a mole fraction of approximately 0.25–0.30, indicating a binding stoichiometry close to 1:2 (HMPP:HPO_4^{2-}).

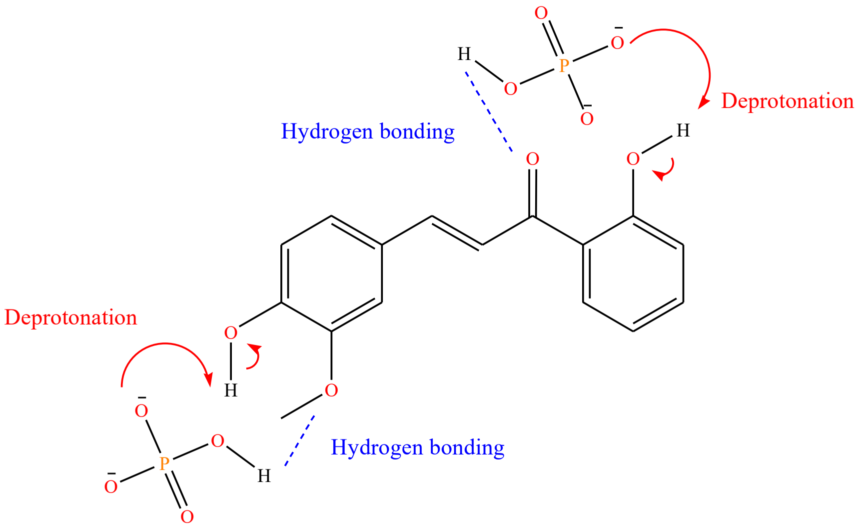

Figure 6. Proposed sensing mechanism of HMPP toward HPO_4^{2-} via hydrogen-bonding interaction and deprotonation. The interaction begins with hydrogen bonding between HPO_4^{2-} and the oxygen-containing functional groups of HMPP, followed by deprotonation of the phenolic –OH groups by HPO_4^{2-}. This process induces electronic redistribution within the conjugated HMPP framework, resulting in a visible color change and enhanced UV–Vis absorbance response toward HPO_4^{2-}.

Selectivity Study

The selectivity of HMPP toward HPO_4^{2-} was evaluated in the presence of various competing anions, including CN^-, Br^-, Cl^-, F^-, and CO_3^{2-}. As shown in the absorbance response (Figure 7), the HMPP–HPO_4^{2-} system exhibited the highest absorbance intensity, indicating a strong and preferential interaction between HMPP and HPO_4^{2-}. The addition of other anions resulted in only minor to moderate changes in absorbance, demonstrating that these species did not significantly interfere with HPO_4^{2-} detection. Although F^- and CO_3^{2-} produced relatively higher responses than the other anions, their absorbance values remained lower than that of HMPP with HPO_4^{2-} alone. These results confirm that HMPP has good selectivity for HPO_4^{2-} over common competing anions and is potentially applicable as a selective colorimetric/UV–Vis chemosensor for phosphate detection. Compared with previously reported phosphate sensors, the selectivity behavior of HMPP is consistent with sensing systems that rely on hydrogen-bonding and charge-transfer interactions. For example, several phosphate sensors based on coordination polymers, metal-complex displacement systems, MOF-based materials, and fluorescent/electrochemical platforms have shown selective responses toward phosphate species, although some of them require metal centers, complex material preparation, or instrumental detection systems[13–24]. In contrast, HMPP provides a simpler chalcone-based colorimetric platform that allows direct visual observation and UV–Vis detection. The lower interference observed from CO_3^{2-}, Cl^-, Br^-, CN^-, and F^- further supports the potential of HMPP as a practical chemosensor for HPO_4^{2-} detection in aqueous samples.

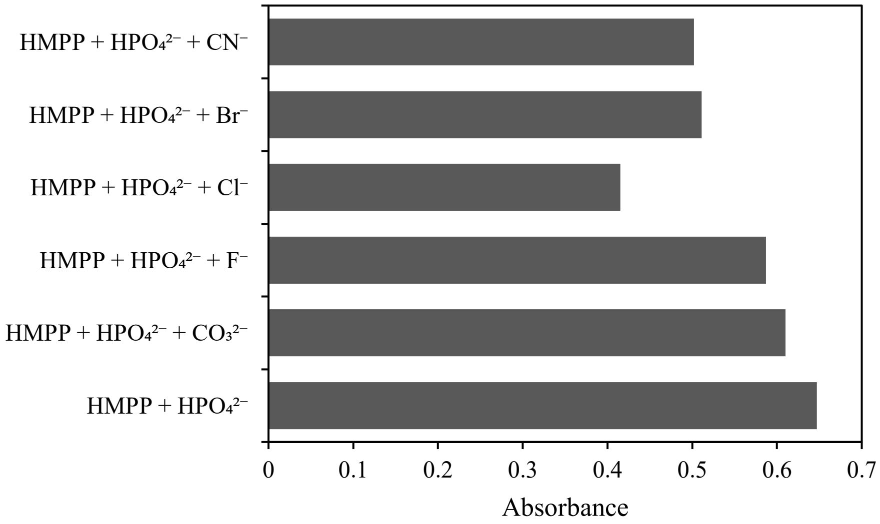

Figure 7. Selectivity study of HMPP toward HPO_4^{2-}. HMPP + HPO_4^{2-} exhibited the highest absorbance compared with systems containing competing anions, indicating good selectivity of HMPP toward HPO_4^{2-}

Table 2. Recovery study of HMPP chemosensor in tap water samples

Sample Location (Coordinate)	Spike Concentration (ppm)	Found Concentration (ppm)	Recovery (%)	Absorbance	Replicate (n=3)	SD	%RSD
Borongpala'la (5°13'06.1"S 119°32'28.6"E)	12.8	13.50	105.47	0.33300	0.326; 0.323; 0.350	0.01480	4.44
Katangka (5°12'31.5"S 119°28'47.0"E)	12.8	13.50	105.47	0.33300	0.314; 0.346; 0.339	0.01682	5.05
Romangpolong (5°12'18.8"S 119°29'47.3"E)	12.8	13.76	107.50	0.33467	0.338; 0.351; 0.315	0.01823	5.45

Application of HMPP Chemosensor in Tap Water Samples

The practical applicability of the HMPP chemosensor was evaluated through recovery studies in tap water samples collected from three different locations in Gowa Regency, South Sulawesi, Indonesia, namely Borongpala'la, Katangka, and Romangpolong villages. The samples were spiked with a known concentration of the target analyte (12.8 ppm), and the recovery performance was assessed using the proposed UV–Vis method.

The obtained results demonstrated satisfactory analytical performance across all sampling sites. In Borongpala'la and Katangka samples, the recovery values were identical at 105.47%, while a slightly higher recovery of 107.50% was observed for the Romangpolong sample. These recovery values fall within the acceptable range for analytical methods (typically 80–120%), indicating good accuracy of the HMPP chemosensor in real sample matrices.

The precision of the method was further evaluated through triplicate measurements. The relative standard deviation (%RSD) values were found to be 4.44%, 5.05%, and 5.45% for Borongpala'la, Katangka, and Romangpolong samples, respectively. These values are below 10%, confirming acceptable repeatability and reliability of the measurement system.

Slight variations in recovery and %RSD among different sampling locations may be attributed to matrix effects, such as the presence of dissolved ions or organic matter in tap water, which can influence the interaction between the analyte and the HMPP sensor. Similar matrix-related effects and environmental sample variations have also been reported in previous studies involving chemical analysis and sensing applications in aqueous systems [34,35]. Nevertheless, the relatively consistent recovery values and low %RSD indicate that such interferences are minimal and do not significantly affect the sensor performance.

Overall, these findings demonstrate that the HMPP-based chemosensor exhibits good accuracy, precision, and robustness for the detection of the target analyte in real water samples. Therefore, it holds strong potential for practical environmental monitoring applications, particularly for rapid and cost-effective analysis of contaminants in aqueous systems.

4. CONCLUSIONS

3-(4-hydroxy-3-methoxyphenyl)-1-(2-hydroxyphenyl)-propenone was synthesized and evaluated as a colorimetric chemosensor for HPO_4^{2-}. The sensor exhibited a distinct color change accompanied by a bathochromic shift, enabling rapid visual and spectroscopic detection. The response was attributed to hydrogen bonding and partial deprotonation of phenolic –OH groups, enhancing π-electron delocalization (ICT). The system showed moderate to good selectivity toward HPO_4^{2-} over competing anions. Application in spiked tap water samples provided satisfactory recoveries (105.47–107.50%) with low %RSD (4.44–5.45%), indicating acceptable accuracy and precision. Although the synthetic yield is moderate (34%), the sensing performance remains effective, highlighting the potential of this chalcone-based system as a simple and cost-effective platform for phosphate detection.

ACKNOWLEDGMENTS

The authors would like to express their sincere gratitude to Ministry of Research, Technology and Higher Education of the Republic of Indonesia (Kemenristekdikti) for the PDD grant contract number 02035/UN4.22.2/PT.01.03/2024 that supported this research. We also extend our appreciation to the Organic Chemistry Laboratory at Hasanuddin University and UIN Alauddin Makassar for providing the necessary facilities and resources. Their support and collaboration were invaluable in the successful completion of this study.

REFERENCES

1. Inobeme A, Natarajan A, Pradhan S, Adetunji CO, Ajai AI, Inobeme J, Tsado MJ, Jacob JO, Pandey SS, Singh KRB, Singh J. Chemical Sensor Technologies for Sustainable Development: Recent Advances, Classification, and Environmental Monitoring. *Adv Sens Res*. 2024;3(12):1-19. doi:10.1002/adsr.202400066
2. Zheng X, Cheng W, Ji C, Zhang J, Yin M. Detection of Metal Ions in Biological Systems: A Review. *Rev Anal Chem*. 2020;39(1):231-246. doi:10.1515/revac-2020-0118
3. Parab H, Ramkumar J, Dudwadkar A, Kumar SD. Overview of Ion Chromatographic Applications for the Analysis of Nuclear Materials: Case Studies. *Rev Anal Chem*. 2021;40(1):204-219. doi:10.1515/revac-2021-0135
4. Edwards N. A New Fluorescent Sensor for the Visual Detection of Anions. *Res Featur*. 2022;(142). doi:10.26904/rf-142-2927566121
5. Pathak AK. Stepwise Hydration of Phosphate Anion: A Microscopic Theory Connecting Domain of Instability and Stability. *Int J Quantum Chem*. 2015;115(7):413-418. doi:10.1002/qua.24816
6. Badamasi H, Nasir M, Ibrahim A, Aliyu I. Impacts of Phosphates on Water Quality and Aquatic Life. *J Water Resour Prot*. 2019;3(12):856-860.
7. Wu Y, Feng J, Hu G, Zhang E, Yu HH. Colorimetric Sensors for Chemical and Biological Sensing Applications. *Sensors*. 2023;23(5). doi:10.3390/s23052749
8. Zeng X, Li X, Sun W. Highly Selective and Sensitive Colorimetric Chemosensor Based on Tricarboyanine for Detection of Ag+ in Industrial Wastewater. *J Leather Sci Eng*. 2020;2(1). doi:10.1186/s42825-020-00031-2
9. González-Vergara A, Sánchez-González R, Bravo MA, Aguilar LF, Espinoza L, Mellado M. Assessment of Chalcone-Vanillin as a Selective Chemosensor of As(III) in Aqueous Solution. *J Mol Struct*. 2022;1266:133558. doi:10.1016/j.molstruc.2022.133558
10. Gupta A, Garg S, Singh H. Development of Chalcone-Based Derivatives for Sensing Applications. *Anal Methods*. 2020;12(42):5022-5045. doi:10.1039/d0ay01603a
11. Fitriana AS, Pranowo HD, Purwono B. Chalcone based colorimetric sensor for anions: Experimental and TD-DFT study. *Indones J Chem*. 2016;16(1):80-86. doi:10.22146/ijc.21181
12. Moon SY, Kim J. Chalcone-Based Colorimetric Chemosensor for Selective Detection of Ni^{2+} Ions. *Chemosensors*. 2022;10(5):151. doi:10.3390/chemosensors10050151
13. Song Y, Zhang J, Wang L, Yang Y. A Europium-Based Coordination Polymer as a Luminescent Sensor for Selective Detection of Phosphate in Aqueous Solution. *RSC Adv*. 2017;7(5):2845-2851. doi:10.1039/C6RA27819A
14. Lohar S, Pal S, Mukherjee M, Chattopadhyay P. A Highly Selective Fluorescent Chemosensor for Phosphate Anions Based on a Zinc(II) Complex. *RSC Adv*. 2017;7(21):12864-12870. doi:10.1039/C7RA02175E
15. Xu F, Leng W, Lu Q, Li K, Zhang Y, Liu J, Xu L, Sheng G. Ratiometric fluorescent sensing of phosphate ion in environmental water samples using flavin mononucleotide-functionalized Fe_3O_4 particles. *Sci Total Environ*. 2023;857:159249. doi:10.1016/j.scitotenv.2022.159249
16. Ben-Aissa S, De Marco R, Susmel S. POM@PMO plastic electrode for phosphate electrochemical detection: A further improvement of the detection limit. *Microchim*

Acta. 2023;190:135. doi:10.1007/s00604-023-05679-1

17. Gupta VK, Jain AK, Maheshwari G, Lang H. Indigo Carmine--Cu(II) Complex as a Dual Colorimetric and Fluorometric Sensor for Phosphate Detection. *Spectrochim Acta Part A Mol Biomol Spectrosc*. 2017;173:762-768.
18. Roy S, Chakraborty A. Fe^{3+} displacement approach for selective colorimetric detection of phosphate ions. *Photochem \& Photobiol Sci*. 2017;16(10):1470-1476. doi:10.1039/C7PP00354D
19. Zhai Y, Li Y, Hou Q, Zhang Y, Zhou E, Li H, Ai S. Highly sensitive colorimetric detection and effective adsorption of phosphate based on MOF-808(Zr/Ce). *New J Chem*. 2022;46:15405-15413. doi:10.1039/D2NJ00640E
20. Kim DY, Kim DG, Jeong B, Kim YI, Heo J, Lee H-K. Reusable and pH-stable luminescent sensors for highly selective detection of phosphate. *Polymers (Basel)*. 2022;14(1):190. doi:10.3390/polym14010190
21. Morgan S, Luy E, Furlong A, Sieben V. A submersible phosphate analyzer for marine environments based on inlaid microfluidics. *Anal Methods*. 2022;14(1):22-33. doi:10.1039/d1ay01876k
22. Altuner EE, Ozalp VC, Yilmaz MD, et al. Development of electrochemical aptasensors detecting phosphate ions on TMB substrate with epoxy-based mesoporous silica nanoparticles. *Chemosphere*. 2022;297:134077. doi:10.1016/j.chemosphere.2022.134077
23. Jeong B, Oh JS, Kim DY, Kim DG, Kim YI, Heo J, Lee HK. Ion-selective electrode based on a novel biomimetic nicotinamide compound for phosphate ion sensor. *Polymers (Basel)*. 2022;14(16):3392. doi:10.3390/polym14163392
24. Chen C, Wiorek A, Gomis-Berenguer A, Crespo GA, Cuartero M. Portable all-in-one electrochemical actuator--sensor system for the detection of dissolved inorganic phosphorus in seawater. *Anal Chem*. 2023;95(8):4180-4189. doi:10.1021/acs.analchem.2c05307
25. Matsjeh S, Swasono RT, Anwar C, Solikhah EN, Lestari E. Synthesis of 2',4-dihydroxy-3-methoxychalcone and 2',4',4-trihydroxy-3-methoxychalcone as a candidate anticancer against cervical (WiDr), colon (HeLa), and breast (T47d) cancer cell lines in vitro. In: *AIP Conference Proceedings*. Vol 1823. ; 2017. doi:10.1063/1.4978121
26. Molbase. 3-(4-hydroxy-3-methoxyphenyl)-1-(2-hydroxyphenyl)prop-2-en-1-one. 2024. https://www.molbase.com/cas/220430-82-0.html.
27. Lusrianti, Balatif N, Zamri A. Sintesis dan uji toksisitas senyawa analog kalkon dari 4'-hidroksiasetofenon dengan dimetoksibenzaldehid. *Phot J Sain dan Kesehat*. 2018;6(01):45-49. doi:10.37859/jp.v6i01.462
28. Nur A, Purwono B. Sintesis kemosensor anion senyawa 4-(2,6-difenil-piridin-4-il)-2-metoksi-fenol dari vanilin. *J Rekayasa Kim \& Lingkung*. 2017;12(1):37-45. doi:10.23955/rkl.v12i1.4957
29. Saifullah MK, Ahasan, Kaleem M, Raneem E, Gupta A, Amir M, A MM, Akhter M, Tasneem S, Shaquiquzzaman. Chalcone derivatives: synthesis, biological evaluation, and structure--activity relationship studies. *Med Drug Discov*. 2025;28:100230.
30. Nematollahi MH, Mehrabani M, Hozhabri Y, Mirtajaddini M, Iravani S. Antiviral and antimicrobial applications of chalcones and their derivatives: From nature to greener synthesis. *Heliyon*. 2023;9(10):e20428. doi:10.1016/j.heliyon.2023.e20428
31. Di Mino C, Clancy AJ, Sella A, Howard CA, Headen TF, Seel AG, Skipper NT. Weak Interactions in Dimethyl Sulfoxide (DMSO)-Tertiary Amide Solutions: The Versatility of DMSO as a Solvent. *J Phys Chem B*. 2023;127(6):1357-1366. doi:10.1021/acs.jpcb.2c07155
32. Jastrzab R, Nowak M, Zabiszak M, Odani A, Kaczmarek MT. Significance and properties of the complex formation of phosphate and polyphosphate groups in particles present in living cells. *Coord Chem Rev*. 2021;435:213810. doi:10.1016/j.ccr.2021.213810
33. Epsztein R, Shaulsky E, Dizge N, Warsinger DM, Elimelech M. Role of Ionic Charge Density in Donnan Exclusion of Monovalent Anions by Nanofiltration. *Environ Sci Technol*. 2018;52(7):4108-4116. doi:10.1021/acs.est.7b06400
34. Wiwit, Ikhsani IY, Nurhamidah, Oktiarni D, Wong KH. Assessment of Macronutrient Dynamics in a Tropical Watershed: A Study from Bengkulu River and Estuary Indonesia. *J Kim Val*. 2025;11(1):41-49. doi:10.15408/jkv.v11i1.42477
35. Ngara ZS, Mamut A, Pingak RK, Johannes AZ, Lerrick RI, Refli. Fabrication and synthesis of fluorescent carbon nanodots from black sticky rice as probes for detection Mg^{2+} ions. *Valensi*. 2025;11(2):162-169.